

Fig. 1

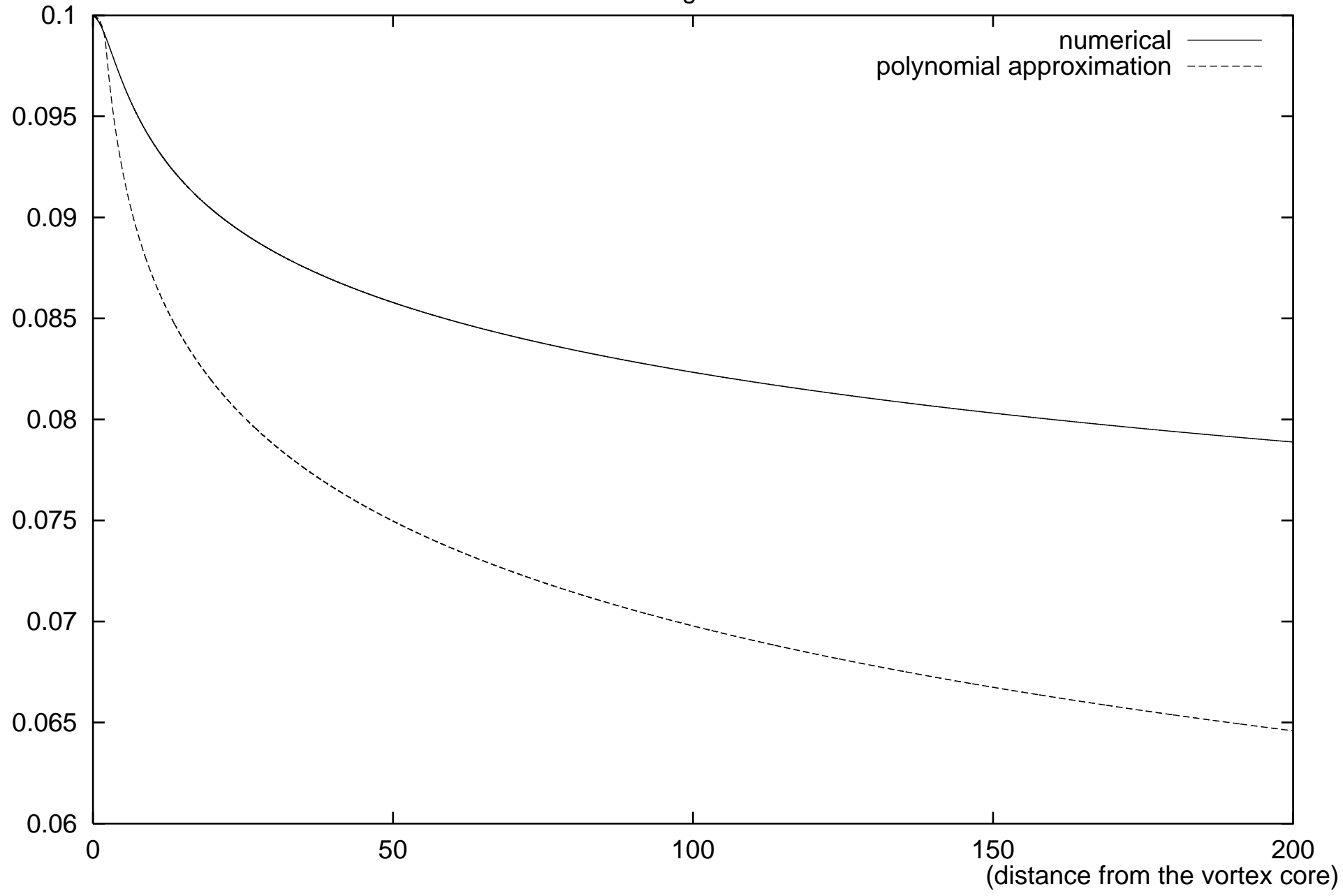


Fig. 2

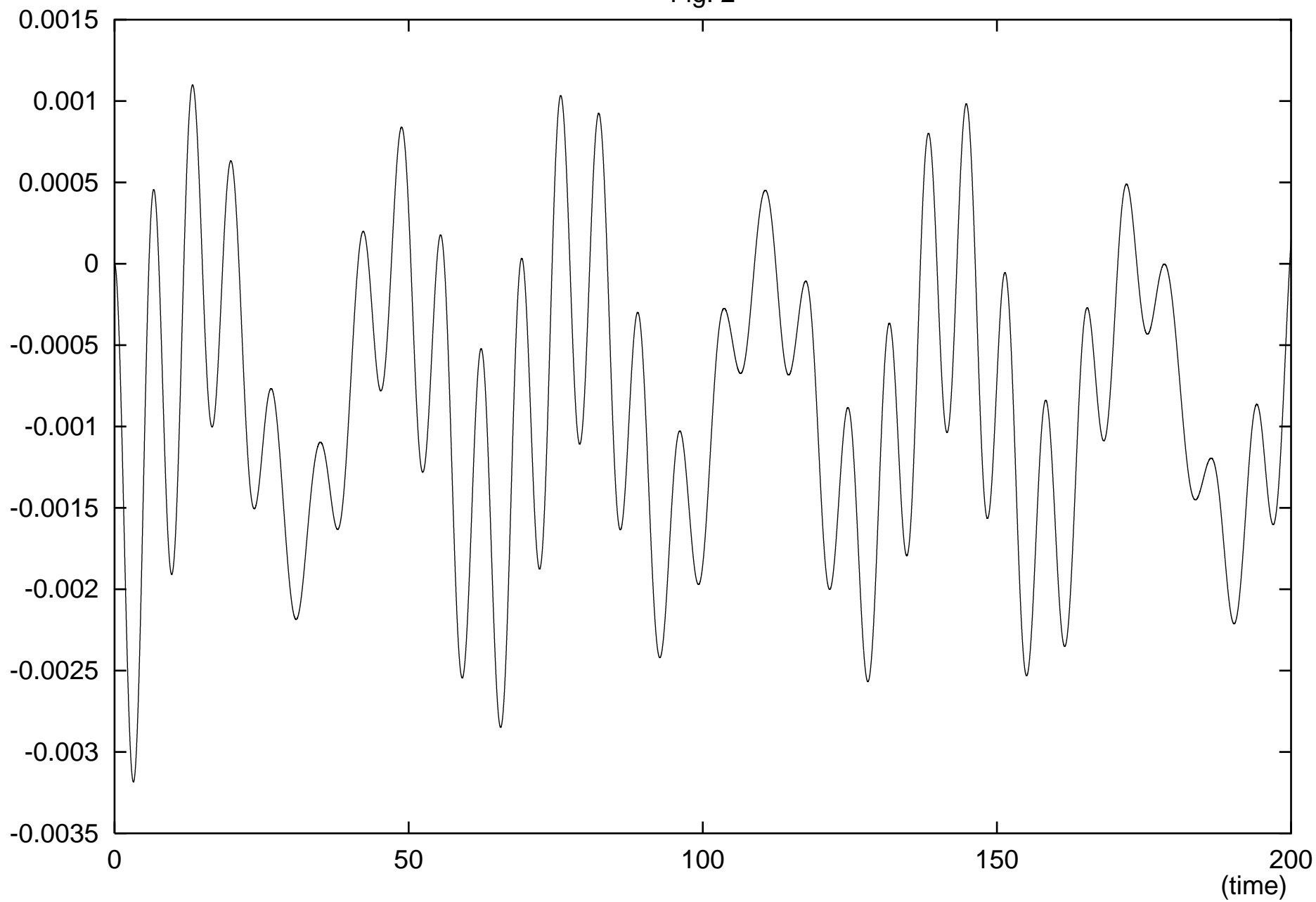


Fig. 3

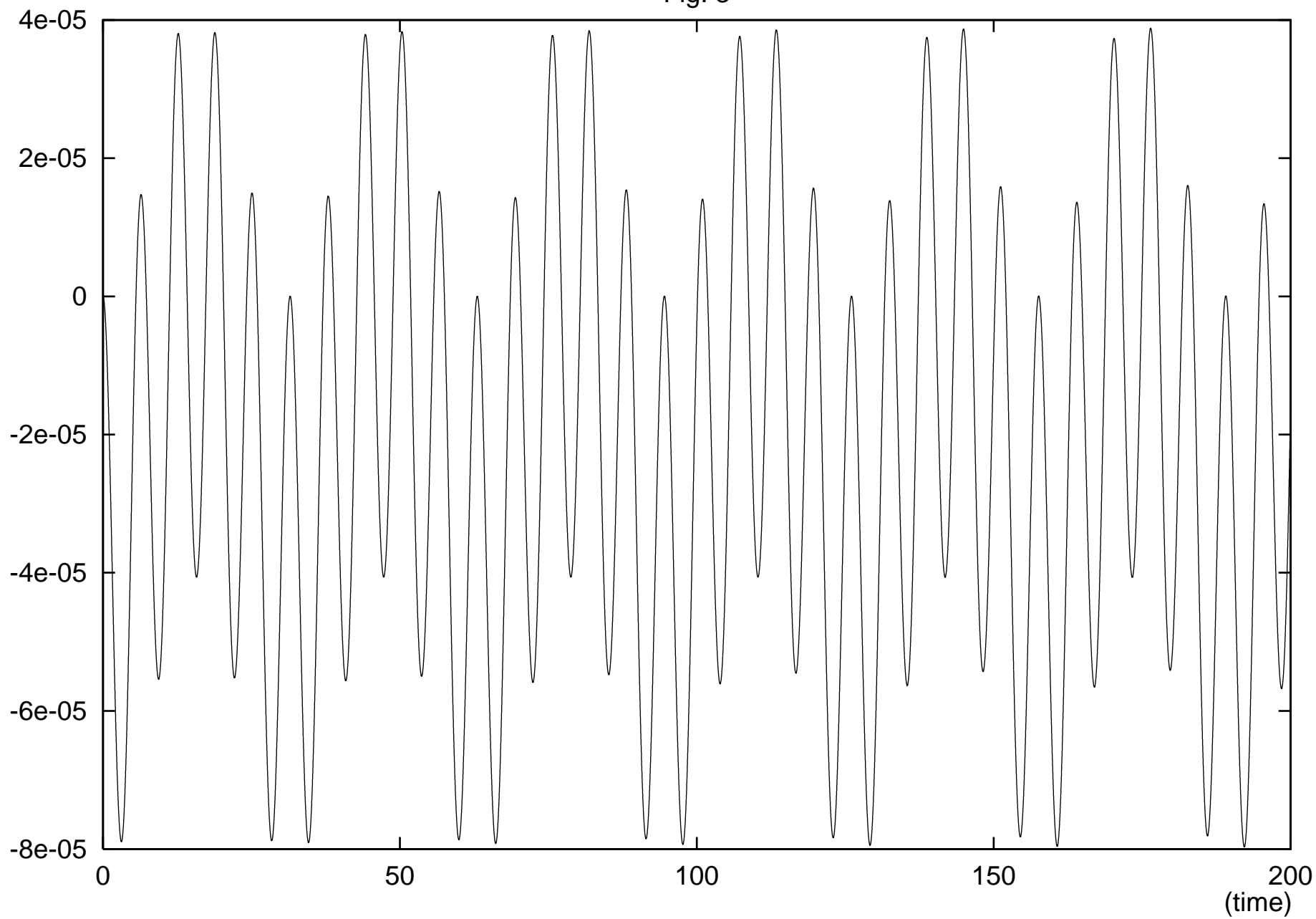


Fig. 4

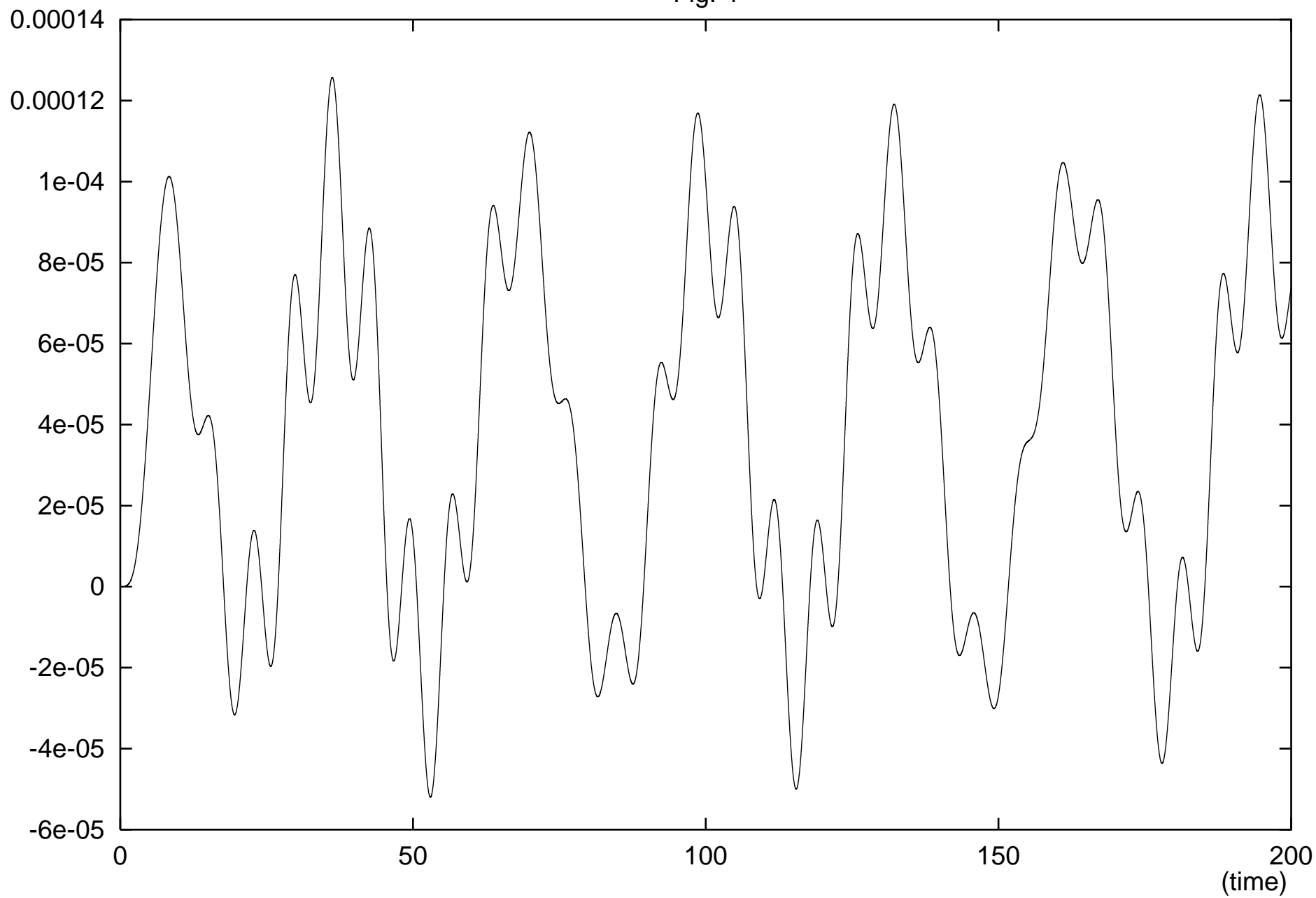


Fig. 5

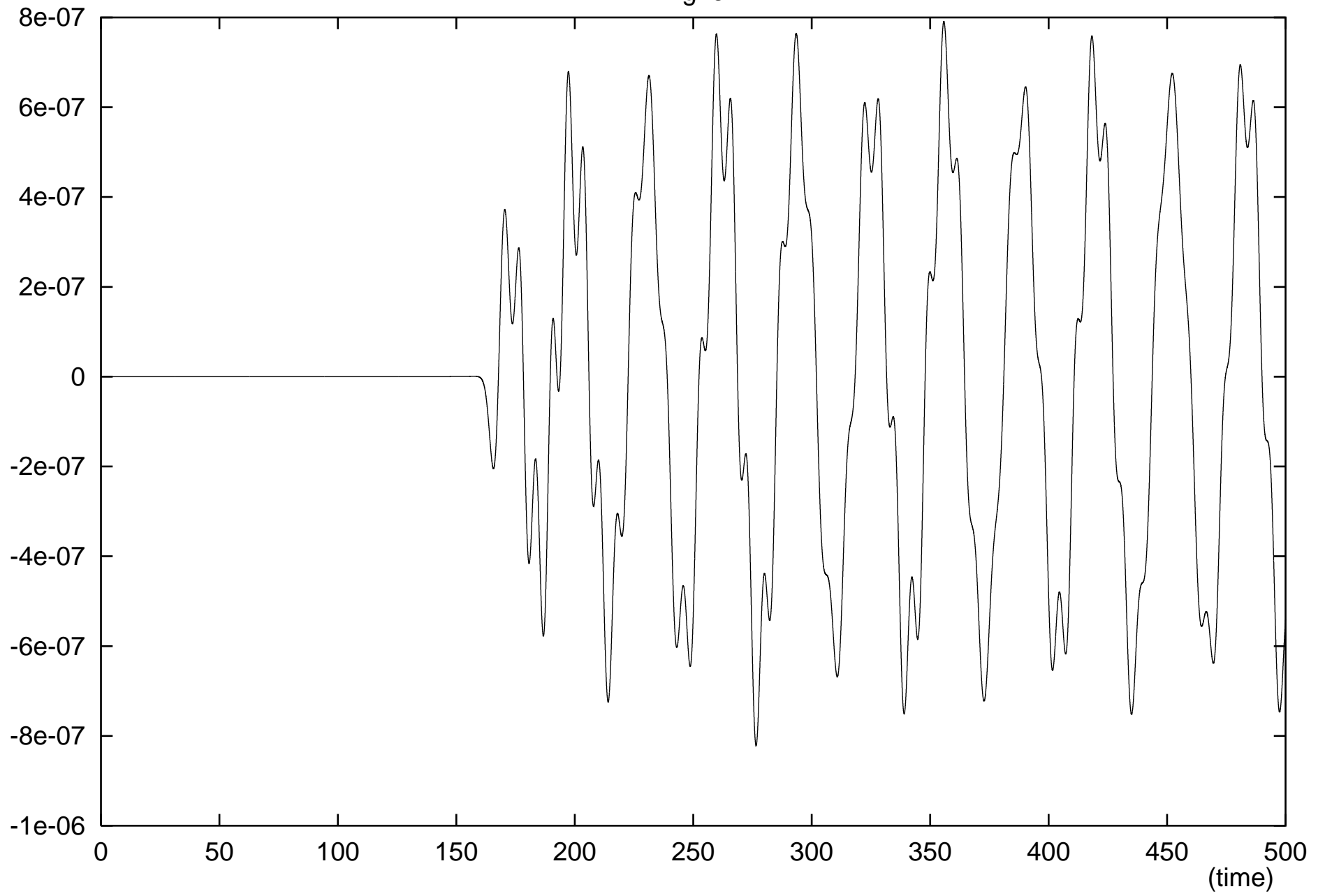


Fig. 6

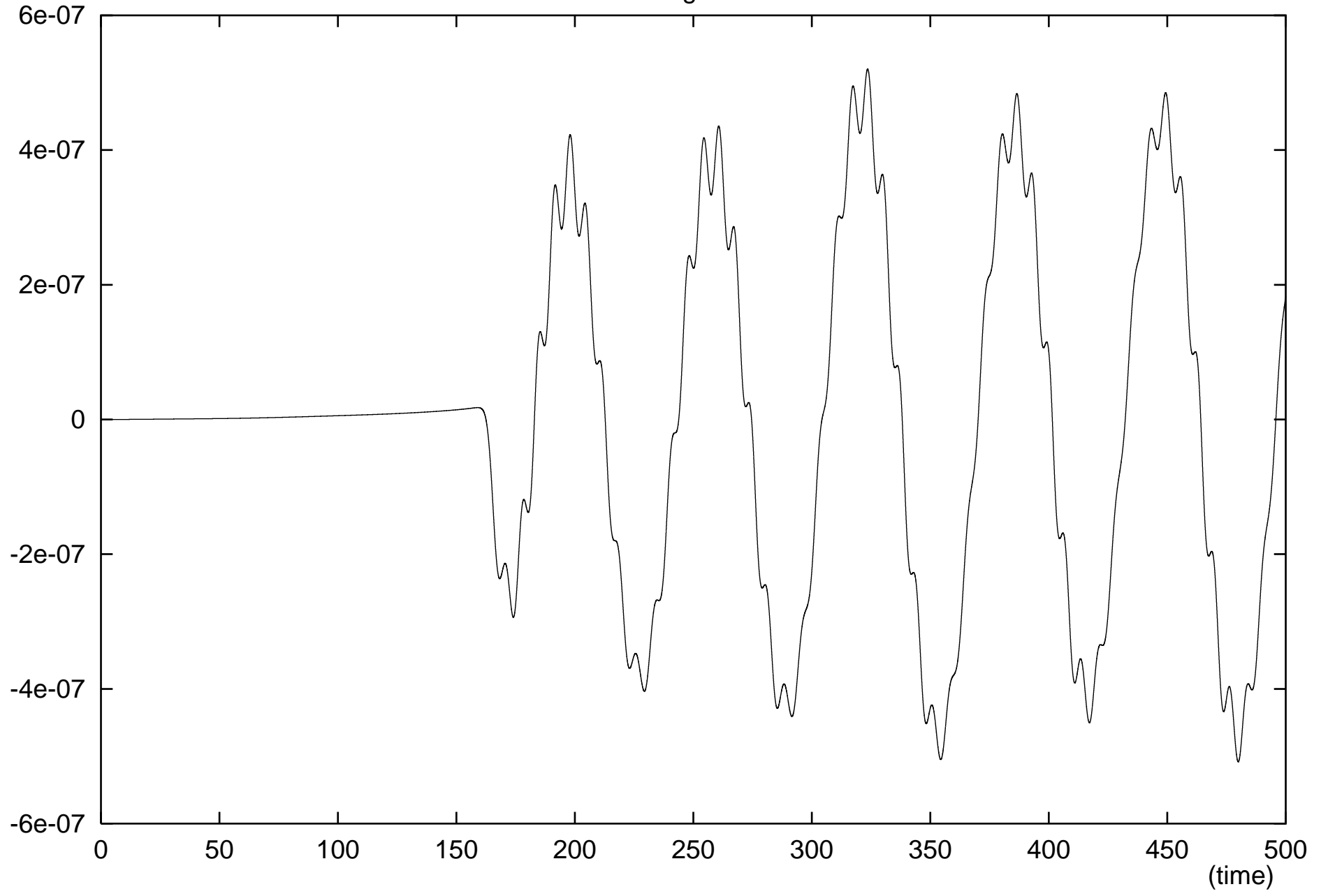


Fig. 7

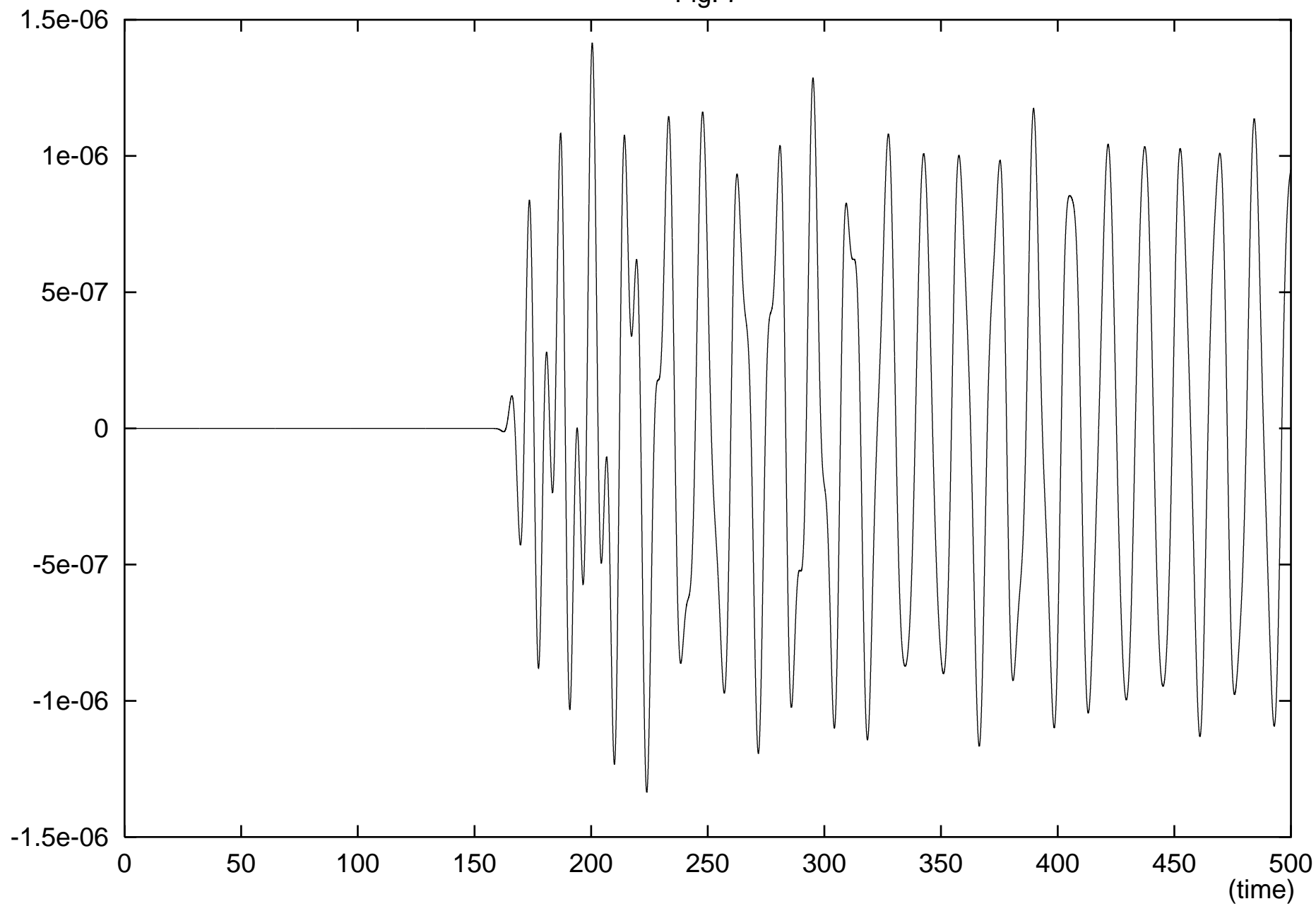


Fig. 8

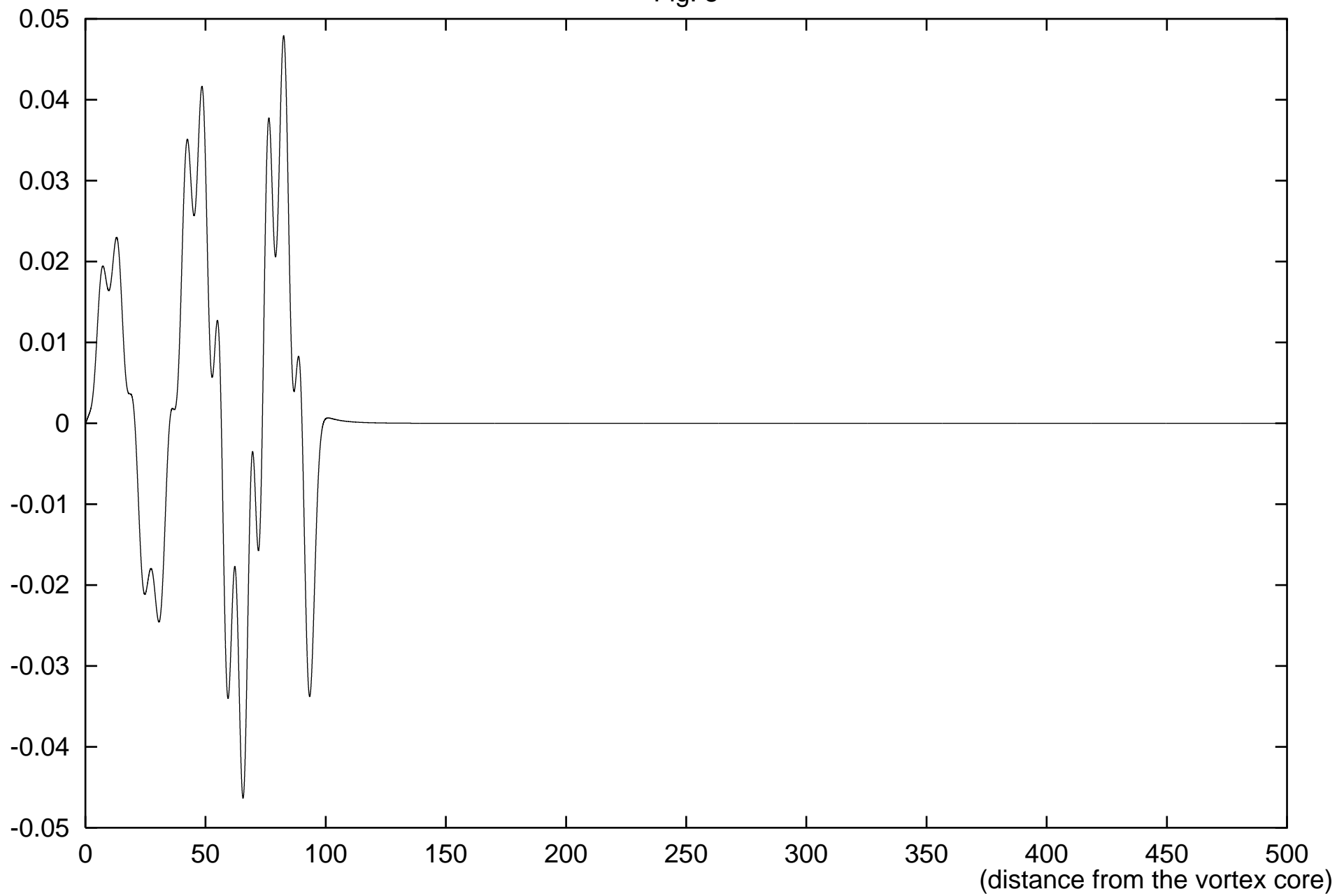


Fig. 9

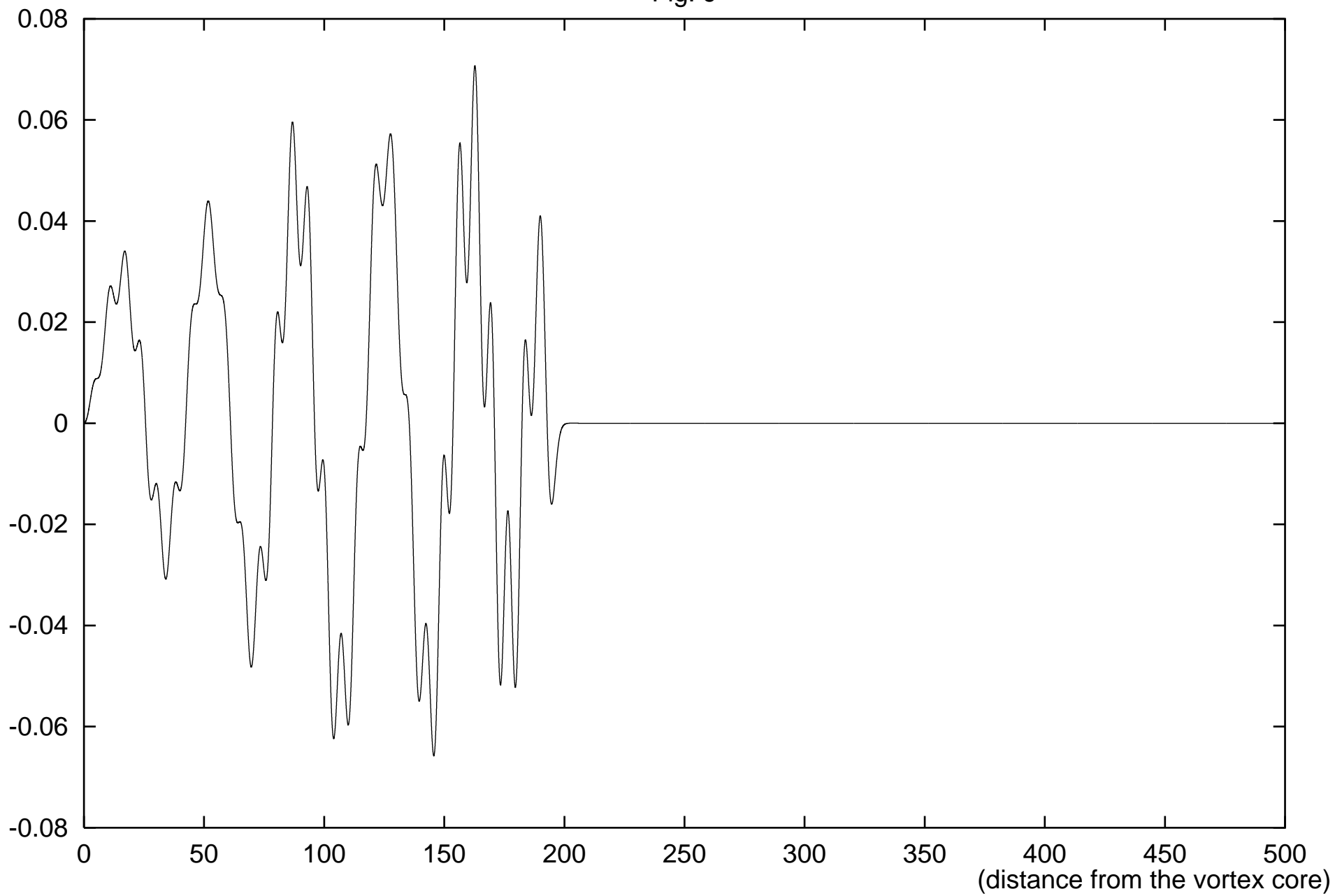


Fig. 10

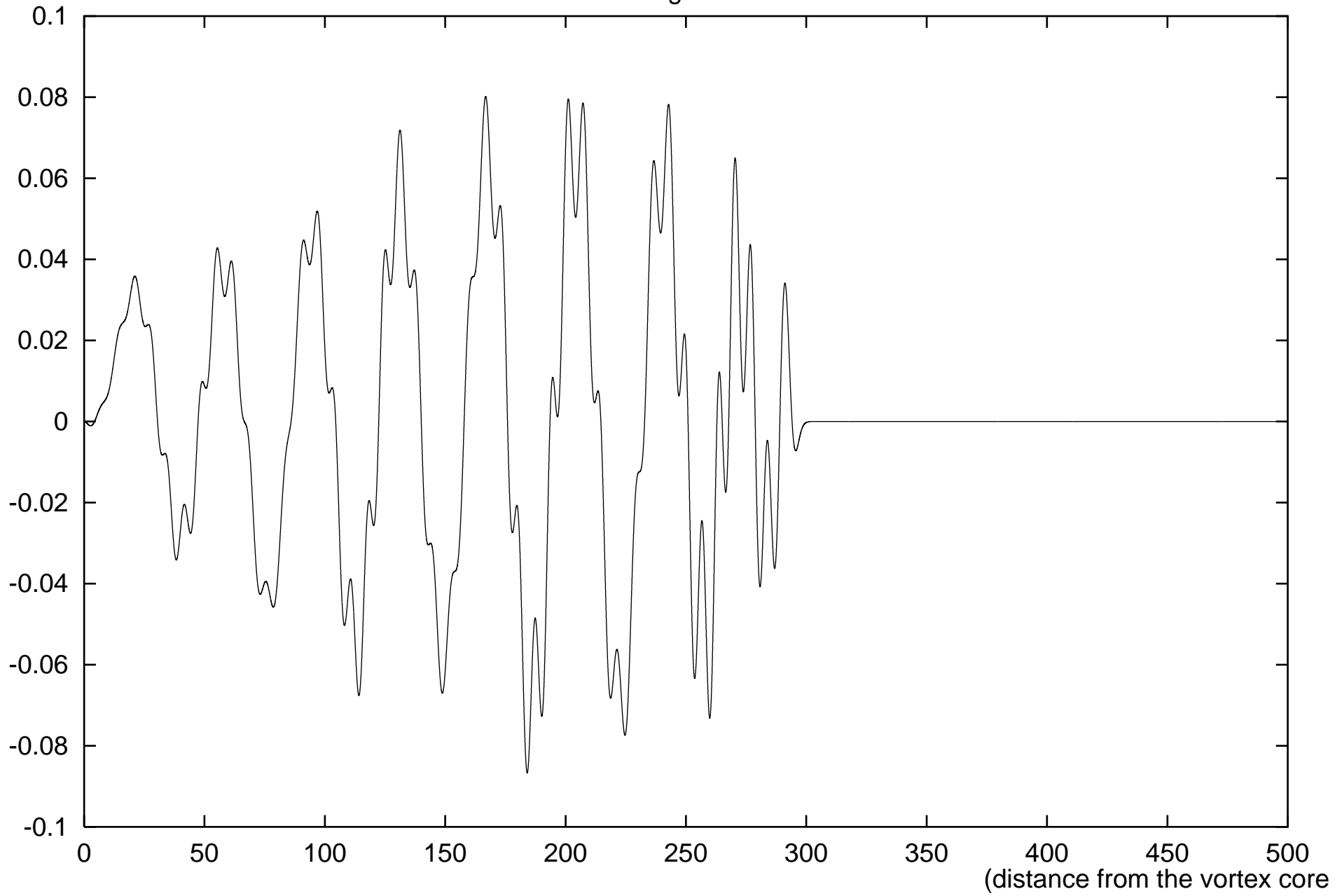


Fig. 11

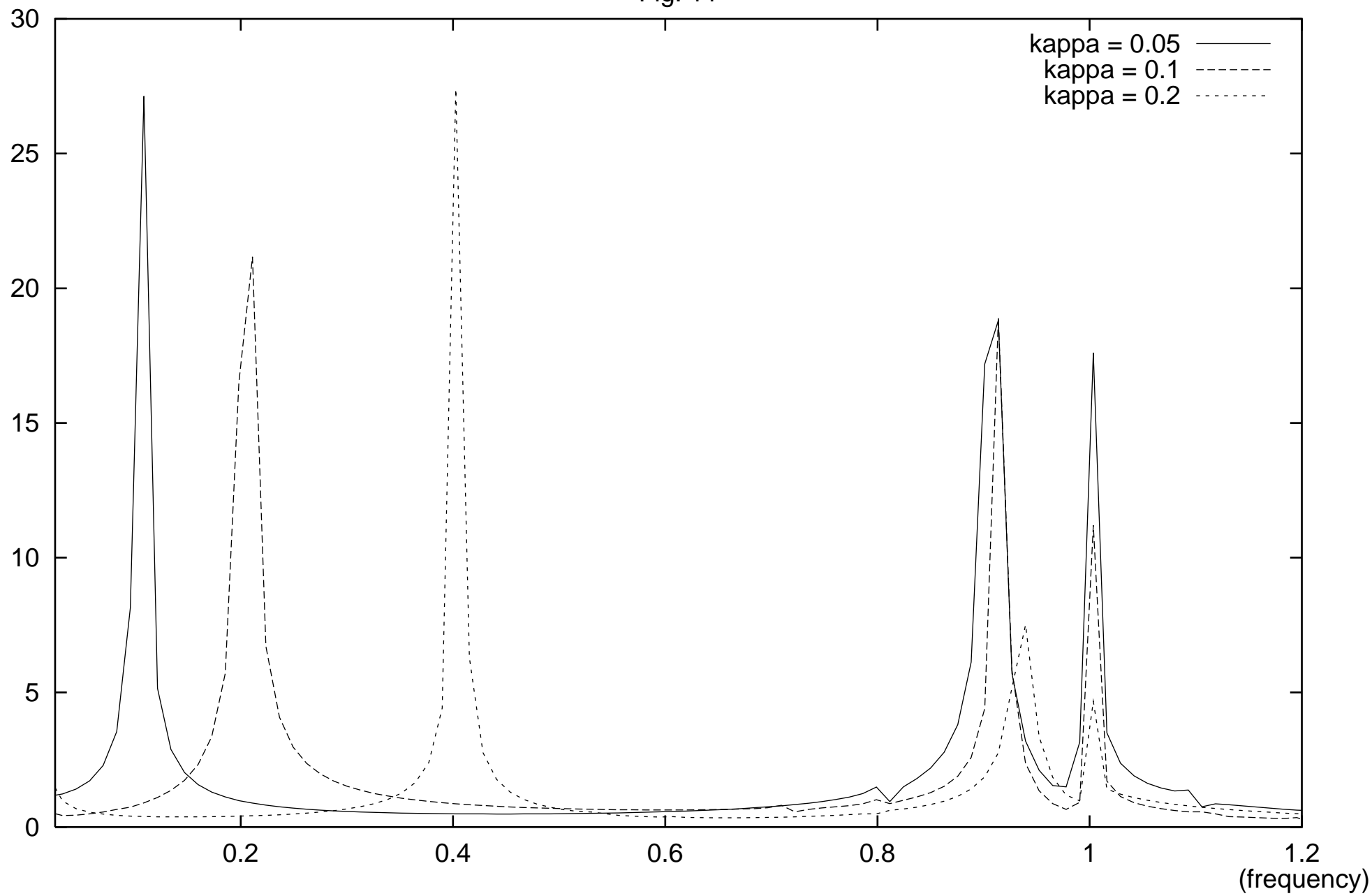


Fig. 12

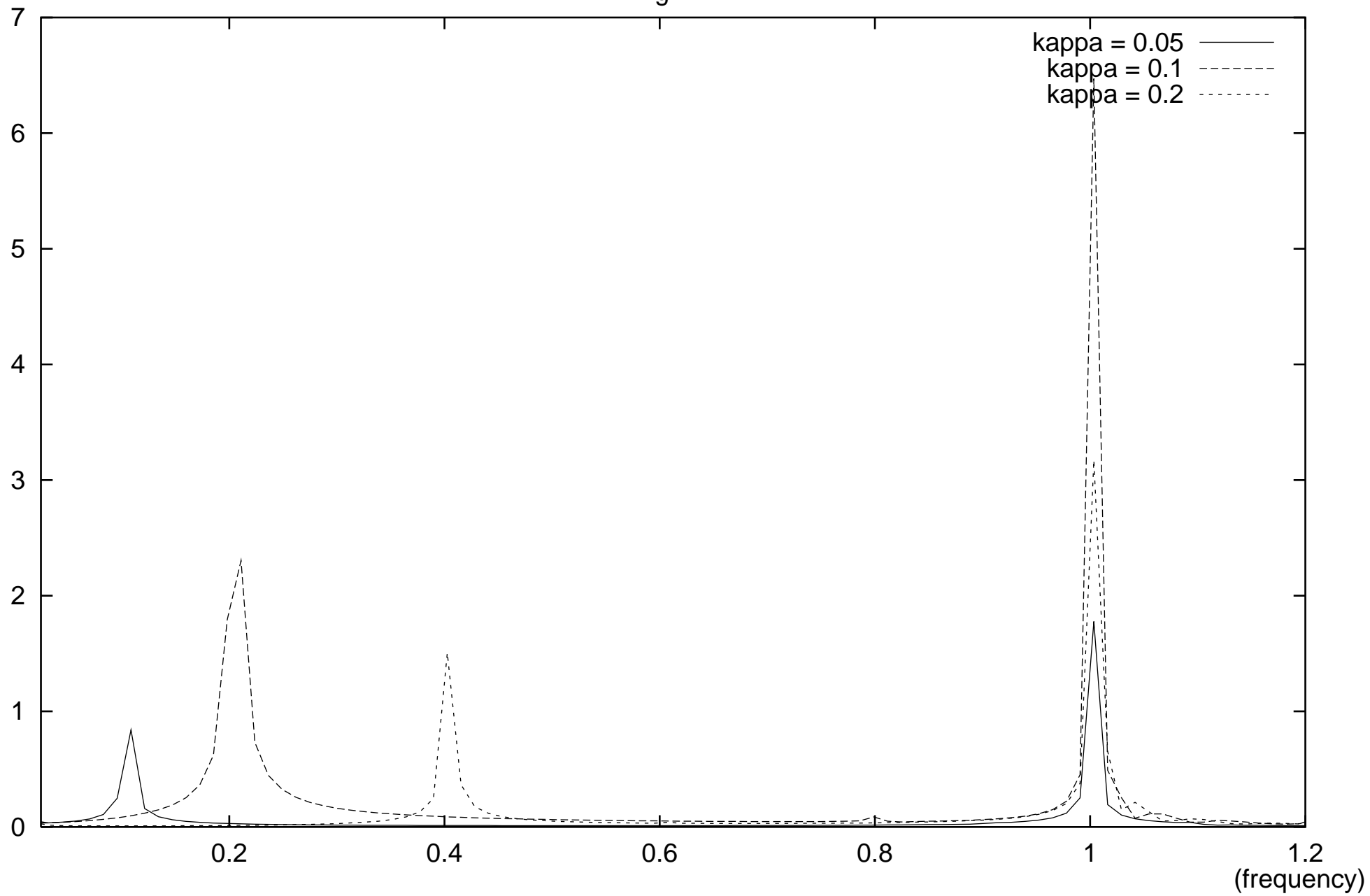


Fig. 13

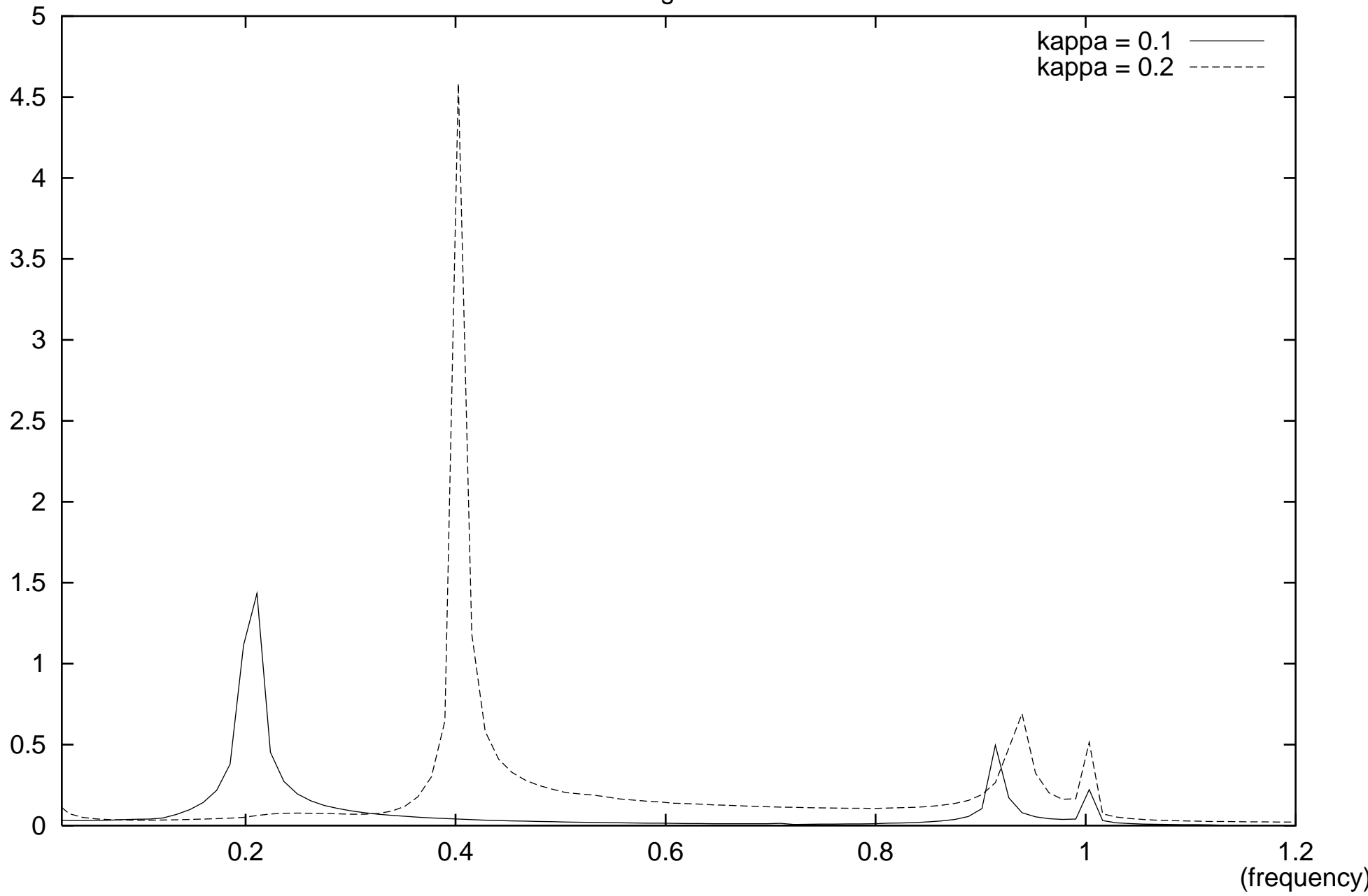


Fig. 14

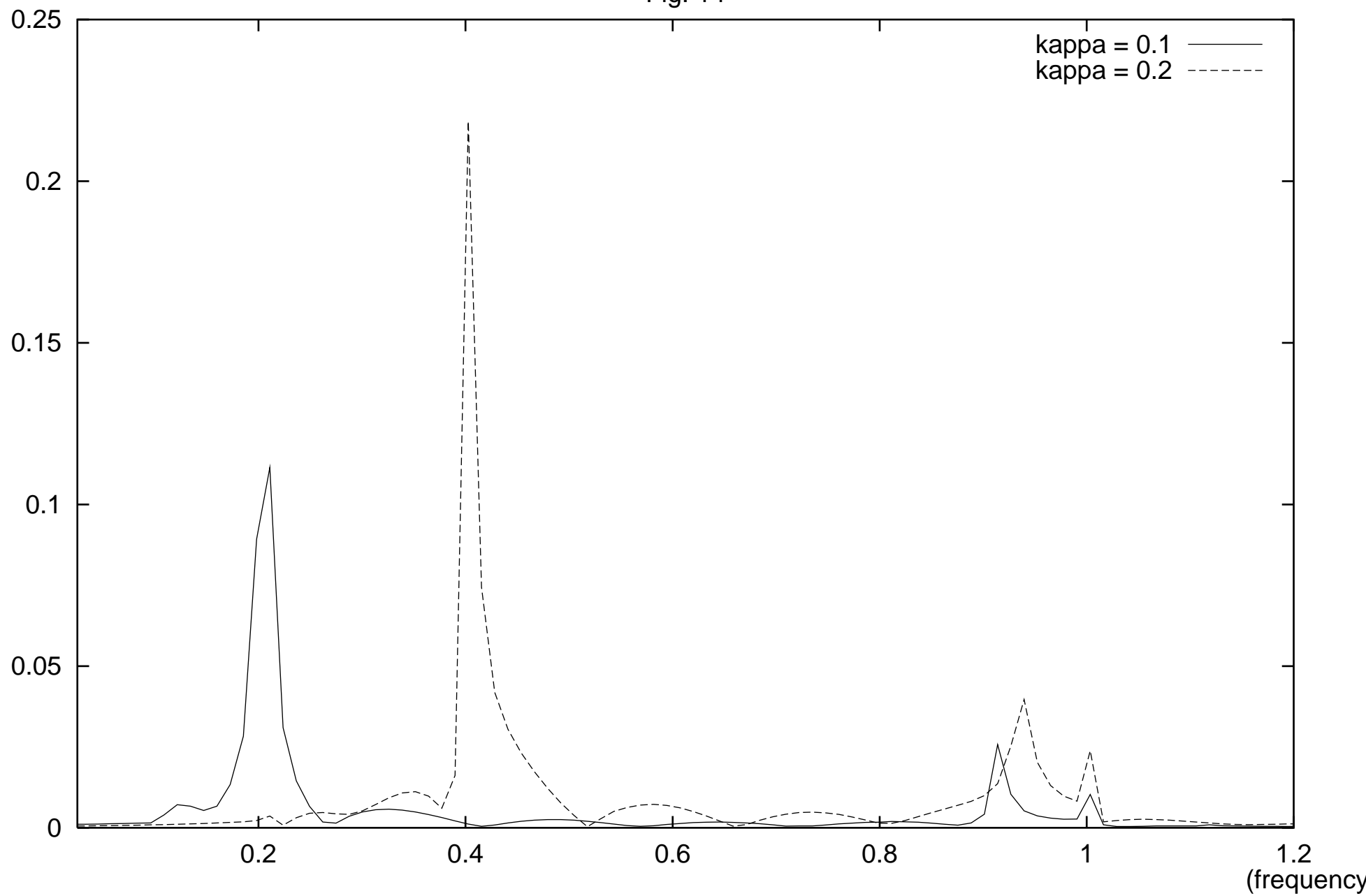


Fig. 15

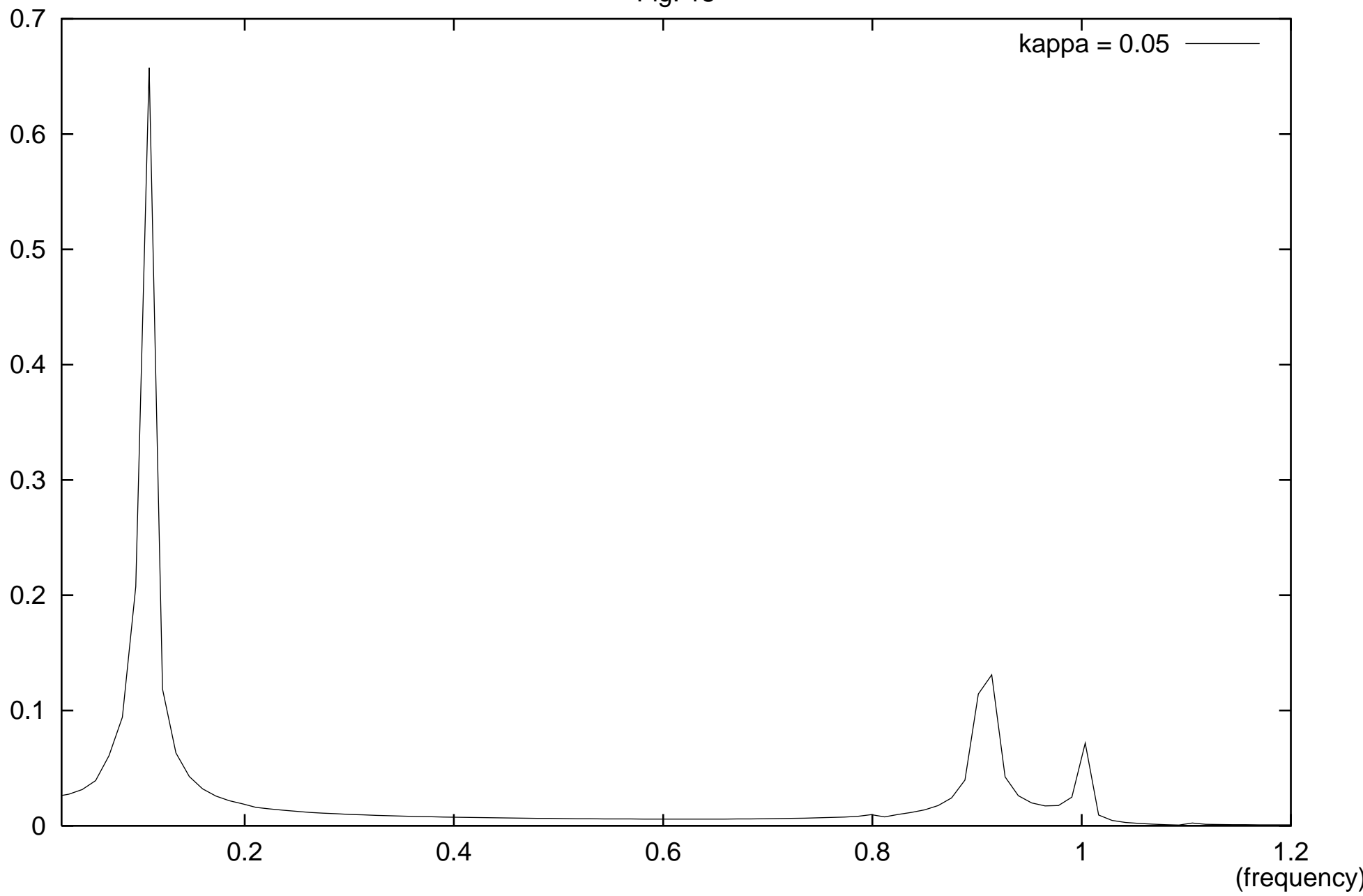


Fig. 16

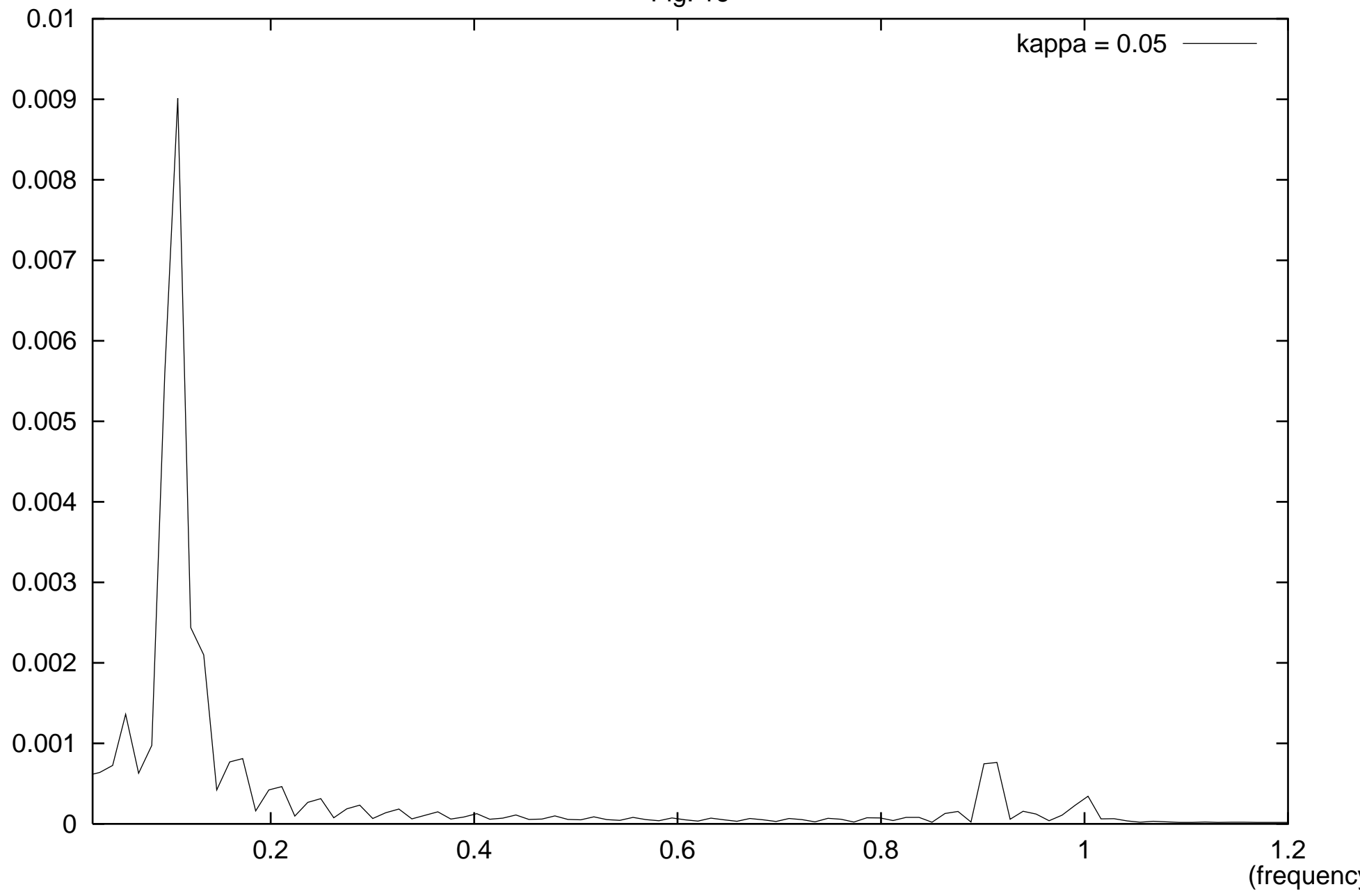


Fig. 1. The initial state of the field A - numerical and polynomial approximations.

Fig. 2. The difference $\delta f_x(t)$ of the dynamical and static values of the field f for $x = 5.0$ and $\kappa = 0.1$.

Fig. 3. The difference $\delta f_x(t)$ of the dynamical and static values of the field f for $x = 160.0$ and $\kappa = 0.1$.

Fig. 4. The difference $\delta h_x(t)$ of the dynamical and static values of the field h for $x = 5.0$ and $\kappa = 0.1$.

Fig. 5. The difference $\delta h_x(t)$ of the dynamical and static values of the field h for $x = 160.0$ and $\kappa = 0.1$. Note the delay time $\approx x$.

Fig. 6. The difference $\delta h_x(t)$ of the dynamical and static values of the field h for $x = 160.0$ and $\kappa = 0.05$. Note the delay time $\approx x$.

Fig. 7. The difference $\delta h_x(t)$ of the dynamical and static values of the field h for $x = 160.0$ and $\kappa = 0.2$. Note the delay time $\approx x$.

Fig. 8. The snapshot of the difference δh_x for $t = 100.0$.

Fig. 9. The snapshot of the difference δh_x for $t = 200.0$.

Fig. 10. The snapshot of the difference δh_x for $t = 300.0$.

Fig. 11. The Fourier transformations modules of the difference $\delta f_x(t)$ for $x = 5.0$ and $\kappa = 0.05, 0.1, 0.2$.

Fig. 12. The Fourier transformations modules of the difference $\delta f_x(t)$ for $x = 160.0$ and $\kappa = 0.05, 0.1, 0.2$.

Fig. 13. The Fourier transformations modules of the difference $\delta h_x(t)$ for $x = 5.0$ and $\kappa = 0.1, 0.2$.

Fig. 14. The Fourier transformations modules of the difference $\delta h_x(t)$ for $x = 160.0$ and $\kappa = 0.1, 0.2$.

Fig. 15. The Fourier transformation modules of the difference $\delta h_x(t)$ for $x = 5.0$ and $\kappa = 0.05$.

Fig. 16. The Fourier transformation modules of the difference $\delta h_x(t)$ for $x = 160.0$ and $\kappa = 0.05$.

The vortex oscillations in Abelian Higgs model

J. Karkowski ^{*} and Z. Świerczyński [†]

October 13, 2018

Abstract

The excitations of the vortex in Abelian Higgs model with small ratio of vector and Higgs particle masses are considered. Three main modes encountered in numerical computations are described in detail. They are also compared to analytic results obtained recently by Arodz and Hadasz [1].

1 Introduction

The vortex type solutions of nonlinear field equations are found to be important in many areas of physics. They are useful in considerations concerning different phenomena in field theory, cosmology and condensed matter physics [2]. However both static and dynamic vortex configurations are known only approximately since they are usually described by complicated non-linear differential equations. Therefore the numerical methods must be applied to examine time-dependent vortex solutions.

The authors of paper [1] have investigated an excitation of the vortex in the Abelian-Higgs model with the mass of the Higgs field much bigger than the mass of the vector particle. They considered time dependent, axially symmetric fields with time and radial components of the gauge potential equal to zero. In the central part of the vortex the fields were approximated by polynomials. These polynomials were continuously matched to the asymptotics describing outer part of the vortex. The authors began with finding an approximation to the static vortex solution. Next they assumed that the evolution of the Higgs field and the azimuthal component of the gauge potential is frozen and considered harmonic oscillations of the gauge potential component parallel to the vortex axis. Finally they found corrections to the Higgs field and the azimuthal component of the gauge potential.

In the present paper we would like to investigate described above excitation of the vortex with the help of numerical computations. We have computed evolution of axially symmetric fields with appropriately chosen initial data. The

^{*}Institute of Physics, Jagellonian University, 30-064 Kraków, Reymonta 4, Poland

[†]Institute of Physics, Pedagogical University, Podchorążych 2, 30-084 Kraków, Poland

approximation used in [1] was simple, and it led to the prediction of oscillations of the Higgs field and of the azimuthal component of the gauge potential with the frequency equal to the doubled frequency of the oscillations of the gauge potential component parallel to the vortex axis. The solutions we have obtained are more complicated. Apart from the predicted mode, they contain also oscillations corresponding to other vortex modes.

Our paper is organized as follows. In Sec. 2 we introduce an axially symmetric ansatz and transform the equations to the form which is more convenient in numerical computations. Sec. 3 has rather technical character: contains description of our computations. The results are presented and discussed in Sec. 4. Finally Sec. 5 involves some general remarks and conclusions summarizing our paper.

2 Abelian Higgs Model

The Abelian Higgs model is described by the following Euler-Lagrange equations

$$(\partial_\nu + iqA_\nu)(\partial^\nu + iqA^\nu)\Phi + \frac{\lambda}{2}\Phi(|\Phi|^2 - \frac{2m^2}{\lambda}) = 0, \quad (1)$$

$$\partial_\mu F^{\mu\nu} = iq(\Phi^* \partial^\nu \Phi - \Phi \partial^\nu \Phi^*) - 2q^2 A^\nu |\Phi|^2. \quad (2)$$

Our notation follows the paper [1]. Here Φ is a complex scalar field, A_ν is $U(1)$ gauge field, m , q , and λ are positive constants. The signature of the metric tensor is $(+, -, -, -)$.

We restrict our considerations to the axially symmetric field configurations described by the following Ansatz

$$\Phi = \sqrt{\frac{2m^2}{\lambda}} e^{i\theta} F(t, r), \quad (3)$$

$$A_0 = 0, \quad A_3 = A(t, r), \quad (4)$$

$$A_1 = \frac{\sqrt{2}m}{qr} \sin \theta (1 - \chi(t, r)), \quad (5)$$

$$A_2 = -\frac{\sqrt{2}m}{qr} \cos \theta (1 - \chi(t, r)), \quad (6)$$

where $r = \sqrt{2m^2((x^1)^2 + (x^2)^2)}$, $\theta = \arctan(x^2/x^1)$, $t = \sqrt{2}mx^0$. The fields have to be non-singular on the x^3 axis. This requirement implies

$$F(t, 0) = 0, \quad \chi(t, 0) = 1, \quad \frac{d}{dr}F(r=0, t) = 0. \quad (7)$$

The axially symmetric ansatz (3)-(6) applied to the equations (1)-(2) simplifies them to the form

$$\ddot{F} = F'' + \frac{1}{r}F' - \left(\frac{1}{r^2}\chi^2 + \frac{q^2}{m^2}A^2 \right) + \frac{1}{2}(F - F^3), \quad (8)$$

$$\ddot{\chi} = \chi'' - \frac{1}{r}\chi' - \kappa^2 F^2 \chi, \quad (9)$$

$$\ddot{A} = A'' + \frac{1}{r}A' - \kappa^2 F^2 A, \quad (10)$$

where dot denotes the time derivative and prime the derivative with respect to the variable r . The dimensionless parameter $\kappa = \sqrt{2q^2/\lambda}$ is equal to the ratio of the vector particle mass and the mass of the Higgs particle. In this paper we restrict ourselves to small values of κ (0.05, 0.1, 0.2). We also assume that $q/m = 1$. This does not limit the generality of our considerations since it can be achieved by rescaling the field A .

Let us note that all field configurations of the form (3)-(6) with finite energy per unit of length in the x^3 direction have unit topological charge. If in addition we assume that the functions f and χ are time independent solutions of the equations (8)-(9) with $A_3 \equiv A \equiv 0$ then we obtain the well known Nielsen-Olesen vortex. This static solution was examined in many papers. However its exact analytical form is not known. Only approximate methods (both analytical and numerical) have been worked out and can be adopted as the starting point to the precise numerical calculations. These are necessary as the time dependent analysis is very subtle.

The equations (8)-(10) are singular in $r = 0$. Therefore we apply to them the following transformation which removes the singularity

$$x = \frac{r^2}{1+r}, \quad (11)$$

$$f(t, x) = \frac{F(t, r)}{r}, \quad (12)$$

$$h(t, x) = \frac{\chi(t, r) - 1}{r^2}, \quad (13)$$

$$a(t, x) = A(t, r). \quad (14)$$

Thus we obtain the equations of the form

$$\begin{aligned} \ddot{f} = & \left(\frac{(2+r)r}{(1+r)^2} \right)^2 f'' + \left(\frac{2}{(1+r)^3} + \frac{2+r}{(1+r)^2} \right) f' \\ & - (2h + r^2 h^2 + a^2) f + \frac{1}{2} f (1 - r^2 f^2), \end{aligned} \quad (15)$$

$$\ddot{h} = \left(\frac{(2+r)r}{(1+r)^2} \right)^2 h'' + \left(\frac{2}{(1+r)^3} + \frac{2+r}{(1+r)^2} \right) h' - \kappa^2 f^2 (1+r^2 h), \quad (16)$$

$$\ddot{a} = \left(\frac{(2+r)r}{(1+r)^2} \right)^2 a'' + \left(2 \frac{(2+r)^2}{(1+r)^3} - \frac{4+r}{(1+r)^2} \right) a' - \kappa^2 r^2 f^2 a. \quad (17)$$

Here prime denotes the derivative with respect to x , $r = \left(x + \sqrt{x(4+x)} \right) / 2$. Some disadvantage of the transformation (11) is that the neighbourhood of the point $r = 0$ is mapped into a very small x interval ($dx/dr|_{r=0} = 0$). Therefore the detailed solution in this region has to be examined separately.

3 The method

In this paper we investigate the oscillations of the vortex caused by the excitations of the field A . The first step is to have the precise solutions for the functions f and χ in the static vortex configuration. In [1] these fields in the central part of the vortex were approximated by polynomials. These polynomials were continuously matched to the appropriate asymptotics describing external part of the vortex. There also exist more precise numerical approximations of the static vortex [3] but their accuracy is not sufficient too. Therefore we have started with one of these approximate methods and then in order to improve the solutions we have applied the average method, that is we have examined the time evolution of the vortex alone averaging the functions f and χ around their equilibrium state.

The next step is to excite the vortex. We have done this by adding a non-zero field A . Following [1] we have used a configuration which gives harmonic oscillations of this field while the vortex fields are frozen. Substituting $A(t, r) = \hat{a}(r) \cos \omega t$ into (10) one obtains

$$\hat{a}'' + \frac{1}{r} \hat{a}' - \kappa^2 F^2 \hat{a} + \omega^2 \hat{a} = 0. \quad (18)$$

As was noticed in [1] this equation has the form of the one-dimensional Schrödinger equation and possesses at least one bound state. Rewriting it in the variable x we obtain

$$\left(\frac{(2+r)r}{(1+r)^2} \right)^2 \frac{d^2 \hat{a}}{dx^2} + \left(2 \frac{(2+r)^2}{(1+r)^3} - \frac{4+r}{(1+r)^2} \right) \frac{d\hat{a}}{dx} - (\kappa^2 r^2 f^2 - \omega^2) \hat{a} = 0. \quad (19)$$

On the uniform grid with the spacing Δ eq. (19) leads to the following finite difference equations

$$\frac{4}{\Delta} (\hat{a}_1 - \hat{a}_0) + \omega^2 \hat{a}_0 = 0, \quad (20)$$

$$\begin{aligned}
& \left(\frac{(2+r)r}{(1+r)^2} \right)^2 \left(\frac{1}{\Delta^2} \right) (\hat{a}_{k+1} - 2\hat{a}_k + \hat{a}_{k-1}) \\
& + \left(2 \frac{(2+r)^2}{(1+r)^3} - \frac{4+r}{(1+r)^2} \right) \frac{1}{\Delta} (\hat{a}_{k+1} - \hat{a}_k) \\
& - (\kappa^2 r^2 f^2 - \omega^2) \hat{a}_k = 0, \quad k = 1, 2, \dots
\end{aligned} \tag{21}$$

For small values of the parameter κ the frequency ω is approximately equal to κ [1]. Therefore we can solve the above difference equations (20), (21) where ω is replaced by κ . We choose arbitrary \hat{a}_0 and successively determine $\hat{a}_1, \hat{a}_2, \dots$. The graphes of the function $A(r) = a(r^2/(1+r))$ obtained from formulae (20), (21) with $\Delta = 0.01$ and the approximation of the function A obtained in the paper [1] for $\kappa = 0.1$ are plotted in Fig 1.

Now we are going to investigate the evolution of the excited vortex using numerical computations. We solve the following finite difference equations

$$\begin{aligned}
f_{j+1,k} &= 2f_{j,k} - f_{j-1,k} + \left(\frac{3}{4} \right)^2 \left(\frac{(2+r)r}{(1+r)^2} \right)^2 (f_{j,k+1} - 2f_{j,k} + f_{j,k-1}) \\
& + \left(\frac{3}{4} \right)^2 \Delta \left(2 \frac{(2+r)^2}{(1+r)^3} + \frac{r}{(1+r)^2} \right) (f_{j,k+1} - f_{j,k}) \\
& + \left(\frac{3}{4} \right)^2 \Delta^2 \left(\frac{1}{2} - 2h_{j,k} - \frac{1}{2}r^2 f_{j,k}^2 - r^2 h_{j,k}^2 - a_{j,k}^2 \right) f_{j,k},
\end{aligned} \tag{22}$$

$$\begin{aligned}
h_{j+1,k} &= 2h_{j,k} - h_{j-1,k} + \left(\frac{3}{4} \right)^2 \left(\frac{(2+r)r}{(1+r)^2} \right)^2 (h_{j,k+1} - 2h_{j,k} + h_{j,k-1}) \\
& + \left(\frac{3}{4} \right)^2 \Delta \left(2 \frac{(2+r)^2}{(1+r)^3} + \frac{r}{(1+r)^2} \right) (h_{j,k+1} - h_{j,k}) \\
& - \left(\frac{3}{4} \right)^2 \Delta^2 \kappa^2 (1 + r^2 h_{j,k}) f_{j,k}^2,
\end{aligned} \tag{23}$$

$$\begin{aligned}
a_{j+1,k} &= 2a_{j,k} - a_{j-1,k} + \left(\frac{3}{4} \right)^2 \left(\frac{(2+r)r}{(1+r)^2} \right)^2 (a_{j,k+1} - 2a_{j,k} + a_{j,k-1}) \\
& + \left(\frac{3}{4} \right)^2 \Delta \left(2 \frac{(2+r)^2}{(1+r)^3} - \frac{4+r}{(1+r)^2} \right) (a_{j,k+1} - a_{j,k}) \\
& - \left(\frac{3}{4} \right)^2 \Delta^2 \kappa^2 r^2 a_{j,k} f_{j,k}^2,
\end{aligned} \tag{24}$$

where Δ is the space between the grid points in the x-direction; the space between time slices is $3\Delta/4$. As the initial values for the fields f and h at $t = 0$

we take found earlier functions corresponding to the static vortex solution. The initial values of the field a are computed from the formulae (20), (21) with $\hat{a}_0 = 0.1$. We also assume that initially the derivatives with respect to time of all fields are equal to zero. In order to remove disturbances of the solution caused by the right boundary of our grid we have performed computations on the larger area and then we removed the part of the grid which could be disturbed.

4 Numerical results

We have computed the evolution of the vortex for $0 \leq t \leq 600$ and $\kappa = 0.05, 0.1, 0.2$ taking $\Delta = 0.01$. The field A oscillates with the frequency $\omega \approx \kappa$. Fig.2-Fig.7 present the evolution of the functions $\delta f_x(t) = f(t, x) - f(0, x)$, $\delta h_x(t) = h(t, x) - h(0, x)$ (i.e. the differences of the time-dependent and static values of the fields f and h respectively) at the points $x = 5$ and $x = 160$. We have chosen these values of the variable x to compare the oscillations near the vortex core with those far from it. The authors of the paper [1] predict oscillations of the field f and χ with the frequency $\omega = 2\kappa$ but they have only analysed the modes forced by the oscillations of the field A . The numerical results we have obtained are more complicated and involve also other vortex modes. These modes will be presented below in more detail. It is also interesting that while the oscillations of the Higgs field f start at once for all values of x the oscillations of the field h are delayed for points far from the vortex centre. They begin at the vortex core and then propagate outside. This fact is also illustrated in Fig.8-Fig.10 which show the plots of the functions δh_x for fixed time values $t = 100, 200, 300$. One can see that in the region $r > t$ the function δh_x is almost equal to zero. It starts to oscillate only when the disturbance of the field h arrives from the vortex centre.

Let us now present the frequencies of the vortex oscillations in the neighbourhood of its equilibrium state. We have computed the fourier transformations for the functions δf_x and δh_x for three different values of κ mentioned above eg. $\kappa = 0.05, 0.1, 0.2$. These calculations have been performed for two distances from the vortex core. As before we have choosen points $x = 5$ and 160 . We have presented our results for the Fourier transformations in Fig.11-Fig.16. The most important conclusions can be summarized as follows. The main frequency of the vortex oscillation is equal to 2κ . The appropriate peak can be easily observed in each of the figures Fig.11-Fig.16. These oscillations are explained in detail in [1] on the basis of the approximate analytic calculations. They are forced by the corresponding oscillations of the field A with frequency κ . But the other vortex modes are also excited. Let us stress that their frequencies do not depend on the parameter κ . The approximate numerical values of these frequencies are correspondingly equal to the mass of the Higgs particle (1.0 in our case) and 90% of this mass (that is 0.9). Let us note that these values seem to be independent from the field a and are two points in the whole spectrum of frequencies of the vortex oscillations computed in [4]. However it is interesting that the lower frequency was not detected for the field f far from the vortex

core (Fig.12).

5 Ending Remarks

The excitation of the vortex we have investigated was obtained by choosing some particular initial data for the component A_z of the gauge field parallel to the vortex axis. In the static vortex solution this component of the gauge field is equal to zero; in our case it oscillates with the frequency approximately equal to κ : the ratio of the vector boson and Higgs masses. The other fields also oscillate. Performing the Fourier transformation we found that the frequencies of these oscillations are grouped near $2\kappa, 0.9, 1.0$. The first value was predicted in [1] and is caused by the term proportional to A^2 in (8). The oscillations with the second frequency appear mainly on the vortex core and are probably concerned with the bound state of the static vortex solution [4]. The third frequency simply equals to the mass of the Higgs particle. However it should be noted that our computations include about ten periods of the field A oscillations and therefore the question concerning the long time behaviour of the system is still open. The field configuration we have considered was constructed in such a way that the field A starts its oscillations at once in the whole space. These oscillations excite the Higgs field for all values of the spatial coordinate. However the motion of the azimuthal component of the gauge field looks differently. It begins at the vortex centre and then propagates outside.

Acknowledgements.

This work was supported in part by KBN grant No. 2 P03B 095 13.

References

- [1] H. Arodź and L. Hadasz, *Phys. Rev. D* **54**, 4004 (1996).
- [2] See e.g. J. S. Ball and F. Zachariasen, *Phys. Rep.* **209**, 73 (1991); C. Olson, M. G. Olson and K. Williams, *Phys. Rev. D* **45**, 4307 (1992); W. B. Kibble, *J. Phys. A* **9**, 1387 (1976); A. L. Vilenkin, *Phys. Rep.* **121**, 263 (1985); R. P. Heubener, *Magnetic Flux Structures in Superconductors*, Springer-Verlag, Berlin - Heidelberg - New York, 1979; R. J. Donally, *Quantised Vortices in Helium*, Cambridge University Press, Cambridge, 1991.
- [3] J. Karkowski, Z. Świerczyński, *Acta Phys. Pol.* **30**, 73 (1999).
- [4] M. Goodband and M. Hindmarsh, *Phys. Rev. D* **52**, 4621 (1995).